Hyperpolarization of "Neat" Liquids by NMR Signal Amplification by Reversible Exchange

ARTICLE *in* JOURNAL OF PHYSICAL CHEMISTRY LETTERS · MAY 2015

Impact Factor: 7.46 · DOI: 10.1021/acs.jpclett.5b00782

9 AUTHORS, INCLUDING:

Thomas Theis
Duke University
28 PUBLICATIONS **299** CITATIONS
SEE PROFILE

Aaron M Coffey
Vanderbilt University
35 PUBLICATIONS **442** CITATIONS
SEE PROFILE

Boyd M Goodson
Southern Illinois University Carbondale
64 PUBLICATIONS **1,536** CITATIONS
SEE PROFILE

Eduard Y Chekmenev
Vanderbilt University
92 PUBLICATIONS **1,767** CITATIONS
SEE PROFILE

THE JOURNAL OF PHYSICAL CHEMISTRY Letters

Letter

pubs.acs.org/JPCL

Hyperpolarization of "Neat" Liquids by NMR Signal Amplification by Reversible Exchange

Roman V. Shchepin,[†] Milton L. Truong,[†] Thomas Theis,[#] Aaron M. Coffey,[†] Fan Shi,[▽] Kevin W. Waddell,[†,§] Warren S. Warren,[#] Boyd M. Goodson,[▽] and Eduard Y. Chekmenev*[,†,‡,∥,⊥]

[†]Institute of Imaging Science, Department of Radiology, [‡]Department of Biomedical Engineering, [§]Department of Physics and Astronomy, [∥]Department of Biochemistry, and [⊥]Vanderbilt-Ingram Cancer Center (VICC), Vanderbilt University, Nashville, Tennessee 37232-2310, United States

[#]Department of Chemistry, Duke University, Durham, North Carolina 27708, United States

[▽]Department of Chemistry and Biochemistry, Southern Illinois University, Carbondale, Illinois 62901, United States

Supporting Information

ABSTRACT: We report NMR Signal Amplification by Reversible Exchange (SABRE) hyperpolarization of the rare isotopes in "neat" liquids, each composed only of an otherwise pure target compound with isotopic natural abundance (n.a.) and millimolar concentrations of dissolved catalyst. Pyridine (Py) or Py derivatives are studied at 0.4% isotopic natural abundance ^{15}N, deuterated, ^{15}N enriched, and in various combinations using the SABRE-SHEATH variant (microTesla magnetic fields to permit direct ^{15}N polarization from parahydrogen via reversible binding and exchange with an Ir catalyst). We find that the dilute n.a. ^{15}N spin bath in Py still channels spin order from parahydrogen to dilute ^{15}N spins, without polarization losses due to the presence of ^{14}N or ^{2}H. We demonstrate $P_{15N} \approx 1\%$ (a gain of 2900 fold relative to thermal polarization at 9.4 T) at high substrate concentrations. This fundamental finding has a significant practical benefit for screening potentially hyperpolarizable contrast agents without labeling. The capability of screening at n.a. level of ^{15}N is demonstrated on examples of mono- and dimethyl-substituted Py (picolines and lutidines previously identified as promising pH sensors), showing that the presence of a methyl group in the ortho position significantly decreases SABRE hyperpolarization.

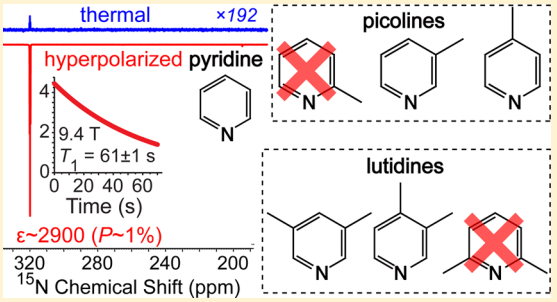

Nuclear spin polarization can be temporarily enhanced by >4 orders of magnitude through the process of *hyperpolarization* with corresponding improvements in sensitivity or signal-to-noise ratio (SNR).[1−3] This significant sensitivity gain can also be used to decrease NMR acquisition time or analyte concentration,[4] but more importantly hyperpolarization techniques enable preparation of large batches of hyperpolarized (HP) compounds, which can be used as contrast agents[5] for various applications involving dynamic tracking in living organisms, including functional pulmonary imaging with HP ^{129}Xe,[3,6] metabolic cancer imaging with HP ^{13}C agents,[7,8] and many others.[9] Advances in hyperpolarization techniques have enabled production of HP agents with sufficient payload (the product of nuclear spin polarization P and concentration/quantity) for in vivo applications and ultimately for human clinical trials, as demonstrated using HP ^{13}C-pyruvate for prostate cancer detection[10] in men and HP ^{129}Xe for lung imaging.[6]

Signal Amplification by Reversible Exchange (SABRE)[11,12] is a particularly cost-efficient and fast hyperpolarization method that relies on exchange of a to-be-hyperpolarized substrate and parahydrogen (*para*-H_2) on a catalyst. Similarly to conventional parahydrogen-induced polarization (PHIP),[13] SABRE utilizes *para*-H_2 as the source of spin order,[14] and the entire hyperpolarization procedure can be completed in seconds; however, unlike PHIP, it does not require the irreversible chemical modification of the substrate.[11,12] Until recently, demonstrations achieving efficient hyperpolarization via SABRE were generally limited to protons; while in some cases the resulting ^{1}H polarization values were relatively high (e.g., $P \approx 8\%$[15]), such nonequilibrium polarization is relatively short-lived (T_1 of seconds). Recent approaches to extend SABRE to longer-lived ($T_1 \approx 1$ min) ^{15}N hyperpolarization include LIGHT-SABRE (Low-Irradiation Generation of High Tesla-SABRE)[16] and SABRE-SHEATH (SABRE in SHield Enables Alignment Transfer to Heteronuclei)[17,18] using RF-irradiation-based and field-cycling-based approaches, respectively. SABRE-SHEATH[17−19] is an advantageous approach because it only requires that the exchange reaction with *para*-H_2 be performed in a microTesla field. This condition can be created easily by shielding the Earth's magnetic field using a mu-metal chamber and is therefore simple and inexpensive. ^{15}N polarization levels

Received: April 14, 2015
Accepted: May 8, 2015
Published: May 8, 2015

DOI: 10.1021/acs.jpclett.5b00782
J. Phys. Chem. Lett. 2015, 6, 1961−1967

of up to 10% were shown in the proof-of-principle demonstration.[17] However, such hyperpolarization was achieved in dilute (4−45 mM) alcohol solutions; that is, the payload (the product of concentration and polarization) of the HP agents was not optimized, and alcohol solutions have limited biocompatibility.

Here, we demonstrate the feasibility of SABRE-SHEATH hyperpolarization of "neat" liquids—each comprised only of an otherwise pure target compound and millimolar concentrations of dissolved catalyst, without any additional diluting solvent. In principle, such liquids could be used directly as hyperpolarized MRI contrast agents; the use of organic solvents is obviated, and we observe greater payload for the concentrated agents.

The previously developed setup for SABRE-SHEATH was utilized,[17,20] wherein *para*-H_2 is bubbled through a liquid agent (e.g., pyridine (Py) or others) containing an activated catalyst (formed from the precursor: [IrCl(COD)(IMes)] (IMes =1,3-bis(2,4,6-trimethylphenyl)imidazol-2-ylidene; COD = cyclo-octadiene)).[15,21] To date, this is the best catalyst for SABRE exchange processes involving *para*-H_2 and the substrate (e.g., Py) shown schematically in Figure 1 (this figure also describes

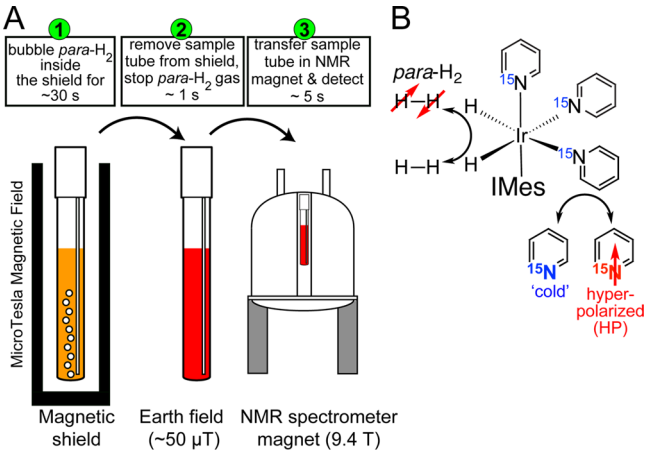

Figure 1. (A) Schematic of the ^{15}N SABRE-SHEATH hyperpolarization process conducted in a pressurized (1−7 atm) 5 mm NMR tube with *para*-H_2 bubbling.[20] (B) Schematic of the SABRE exchange process, wherein parahydrogen and a substrate, for example, pyridine, exchange on activated Ir-hydride complexes.[15]

the sample manipulation during ^{15}N SABRE-SHEATH process). Proton hyperpolarization via SABRE at milliTesla magnetic fields (6 ± 4 mT) was performed as described previously,[20,22] with *para*-H_2 bubbling performed in the fringe field (6 ± 4 mT) of the 9.4 T magnet (instead of steps 1 and 2 shown in Figure 1A). See the Supporting Information (SI) for additional experimental details. We note that SABRE of protons is most efficient in the milliTesla regime, whereas SABRE of ^{15}N spins is most efficient in microTesla fields,[17] as dictated by the respective matching conditions requiring that the frequency differences between the source and target spins be reduced to roughly match the scalar couplings between them.

When neat natural abundance (n.a.) Py was used for ^{15}N SABRE-SHEATH, large ^{15}N signal enhancements (ε up to 2900) were observed, corresponding to $P_{15N} \approx 1\%$ (Figure 2A). Remarkably, ^{1}H SABRE (conducted conventionally at ∼6 mT field[15]) yielded very small signal enhancement of $\varepsilon \approx 4$ (Figure 2B). The ^{15}N signal exhibited a strong, nearly linear dependence on the flow rate of *para*-H_2 in the range studied (the flow-rate of 150 standard cubic centimeters (sccm) represents an experimental limitation of our setup at ∼7 atm), which was metered independently of the applied pressure and hence solution *para*-H_2 concentration (Figure 2C). Note that the ^{15}N signal enhancement was approximately independent of the *para*-H_2 pressure (and solution concentration according to Henry's law), indicating that the flux of the available *para*-H_2 spin bath (the source of spin order) was indeed the limiting factor; that is, the potential possibility of exchanging more *para*-H_2 per unit time would likely yield greater ^{15}N signal enhancements. Larger *para*-H_2 exposure can be attained by higher pressures and smaller bubbles/better gas-phase−liquid-phase mixing.

The other important effect limiting the maximum achievable hyperpolarization is spin−lattice relaxation. The ^{15}N spin−lattice relaxation time is significantly shorter in microTesla fields than at high field (9.4 T), 5.5 ± 0.5 versus 60.8 ± 0.6 s, respectively (Figures 2E,F), and such efficient relaxation results in SABRE-SHEATH ^{15}N enhancements reaching significantly lower steady-state levels after the hyperpolarization procedure. More importantly, the supply of *para*-H_2 is limited because only ∼0.1 mmol/s pass through the tube at the maximum flow rate of 150 sccm, whereas 90 mM catalyst (in ∼0.4 mL volume) alone is capable of exchanging of ∼0.2 to 0.4 mmol/s of H_2 because the hydrogen exchange rate is ∼5−10 per s.[23] However, Ir-hydride protons do not have 100% exchange efficiency with *para*-H_2 gas. Instead, this exchange is further constricted by at least two major bottlenecks: (i) exchange of H_2 between gas and liquid phases and (ii) exchange of dissolved *para*-H_2 with Ir-hydride. Note that equilibrium H_2 concentration in organic solvents is <4 mM/atm;[24−26] that is, even at the maximum *para*-H_2 pressure used (∼7 atm), *para*-H_2 concentration is <30 mM, that is, at least three times lower than that of the Ir-hydride catalyst at 90 mM concentration. Moreover, when *para*-H_2 singlet spin order is transferred to Py via SABRE, *para*-H_2 becomes *ortho*-H_2, manifesting as an HP byproduct,[22] and this resulting *ortho*-H_2 can no longer serve as a source of hyperpolarization in conventional ex situ SABRE. Furthermore, hydride proton exchange rates are on the order of 10 per second;[23] therefore, each *para*-H_2 molecule on average experiences >30 exchanges per second under these conditions ([catalyst] of ∼90 mM results in the total of ∼900 *para*-H_2 exchanges per second for <30 mM [*para*-H_2] dissolved). The main implication of the above two bottlenecks, the fast hydrogen exchange and the limited flux of *para*-H_2 gas, is that [*ortho*-H_2] ≫ [*para*-H_2]. Furthermore, the additional feature of the complex interplay of microTesla ^{15}N effective T_1 and limited access to *para*-H_2 is that it should imply the existence of an optimal catalyst concentration and an optimal ratio of Py to catalyst concentrations. Taken together, these results indicate that greater signal enhancements are potentially feasible, provided that engineering issues limiting *para*-H_2 access for SABRE hyperpolarization are solved.

The additional evidence that the finite *para*-H_2 spin bath is limiting the SABRE processes is also seen when n.a. Py ($\varepsilon \sim$ 2900) was replaced by 99% ^{15}N enriched Py (^{15}N-Py, $\varepsilon \approx 33$), Table 1. ^{15}N signal enhancement decreases by nearly 2 orders of magnitude (88-fold), while the concentration of ^{15}N spins is increased by 278 fold (= 1/0.0036); however, note that the total Py concentration and quantity is maintained the same. In summary, the observed signal (given by the product of [^{15}N] and ε) only decreases by 3 fold when working with n.a. Py.

DOI: 10.1021/acs.jpclett.5b00782
J. Phys. Chem. Lett. 2015, 6, 1961−1967

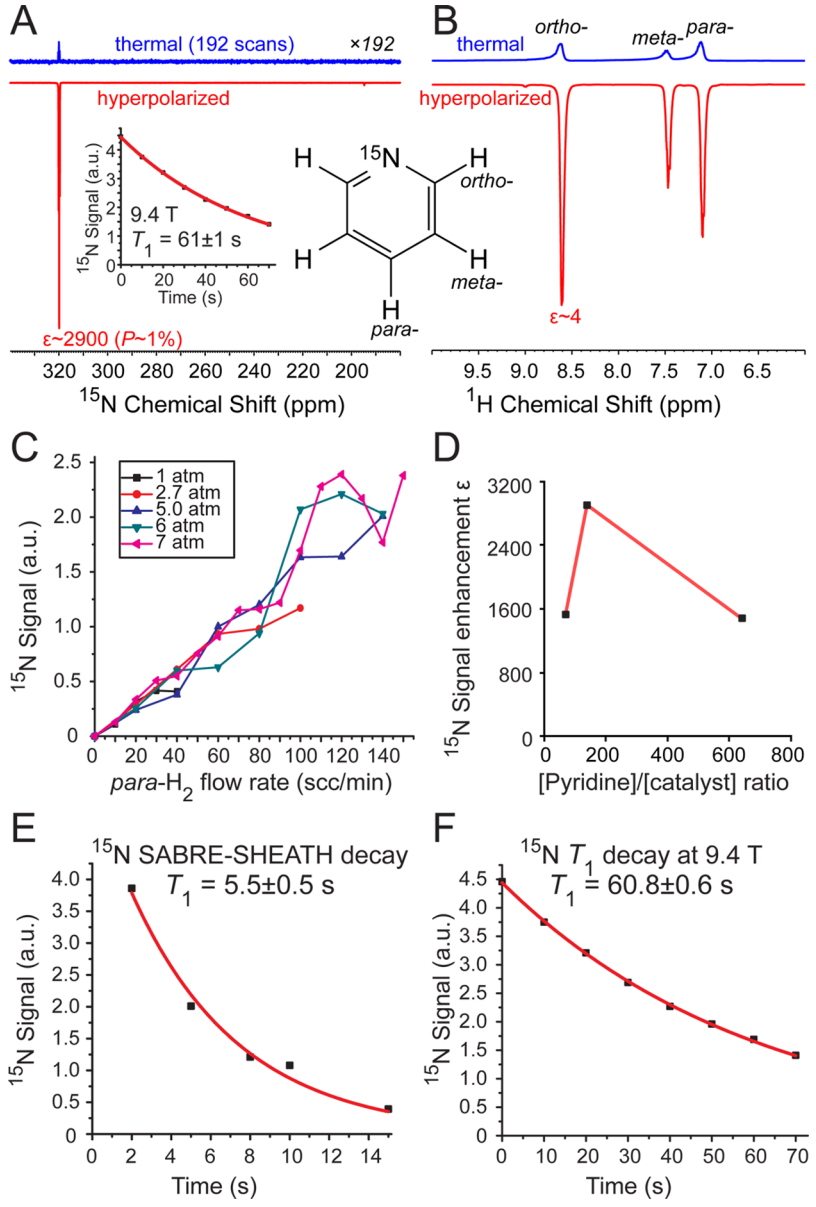

Figure 2. SABRE of "neat" natural abundance ^{15}N (0.36%) pyridine (Py). (A) ^{15}N SABRE-SHEATH hyperpolarized spectrum (red) and the corresponding thermally polarized reference spectrum (blue) after 192 signal averages. (B) ^{1}H SABRE spectrum of hyperpolarized (red) sample in milliTesla magnetic field (~6 mT) and the corresponding NMR spectrum using thermally polarized sample (blue). (C) Effect of the *para*-H_2 flow rate (measured in standard cubic centimeters per minute or sccm) on ^{15}N signal enhancement at ~90 mM catalyst concentration under five *para*-H_2 pressure values. (D) Effect of [Py] to [catalyst] ratio on ^{15}N signal enhancement using 120 sccm flow rate under ~7 atm of *para*-H_2 pressure. (E) ^{15}N SABRE-SHEATH dependence (modeled as exponential decay) as a function of the sample exposure to the microTesla magnetic field after stopping *para*-H_2 bubbling time. (F) ^{15}N T_1 decay at 9.4 T. The experiments in panels E and F are conducted using ~90 mM catalyst concentration (~140:1 [Py] to [catalyst] ratio) at 120 sccm flow rate and ~7 atm *para*-H_2 pressure.

Another important aspect in this context is that ^{15}N microTesla effective T_1 of ^{15}N-Py (10.2 ± 1.1 s) is actually longer than that of n.a. Py (5.5 ± 0.5 s); see Table 1.

Furthermore, achieving such significantly greater (by 88-fold) ^{15}N ε in n.a. Py with respect to ^{15}N-Py under the conditions of limited access to *para*-H_2 has a major significance for the mechanistic understanding of the SABRE-SHEATH phenomenon. In particular, this result indicates that the hyperpolarization *para*-H_2 spin bath is not depleted when the exchanging substrate on Ir-hydride catalyst is ^{14}N-Py. If no interaction between *para*-state of hydride and ^{15}N-Py occurs (i.e., the exchanging partner is ^{14}N-Py), *para*-state of hydride should exchange back into *para*-H_2 with preservation of the *para*-H_2 hyperpolarization pool (Figure 4B). This is an important conclusion because the spin order residing in the entire pool of *para*-H_2 can be selectively channeled to hyperpolarize ^{15}N nuclei of the exchangeable substrate (e.g., n.a. Py) rather than (say) being depleted by rapidly relaxing ^{14}N sites acting as hyperpolarization sinks. This finding fundamentally enables achieving relatively high levels of ^{15}N hyperpolarization (e.g., $P_{15N} \approx 1\%$), even when performing SABRE-SHEATH in the high substrate concentration regime encountered with effectively neat solutions and when the supply and transport of *para*-H_2 are restricted. The ^{14}N species likely do not deplete the *para*-H_2 state because the quadrupolar relaxation rate of the ^{14}N spins is faster than the *J*-coupling

DOI: 10.1021/acs.jpclett.5b00782
J. Phys. Chem. Lett. 2015, 6, 1961−1967

Table 1. Summary of Experimental Results with Natural Abundance (n.a.) Pyridine (Py), Py-d_5, ^{15}N-Py, and Their Mixtures[a]

	[^{15}N] (mM)	^{15}N ε @ 9.4T	^{15}N effective T_1 μT (s)	^{15}N T_1 9.4T (s)	*ortho*-[^{1}H] (mM)	^{1}H ε @ 9.4T	[catalyst] (mM)
1) Py (n.a.)[b]	~45	~−2900	5.5(0.5)	60.8(0.6)	~25000	~−4.2	~90
2) Py-d_5 (99.5% d)	~45	~−850	2.2(0.1)	74.3(2.9)	~125	~−60	~90
3) ^{15}N-Py	~12500	~−33	10.2(1.1)	66.8(0.5)	~25000	~−0.3	~90
4) catalyst activated with ^{15}N-Py, then Py-d_5 added	~2000	~−520	10.1(0.8)	69.9(0.3)	~4000	~−2.6	~90
5) catalyst activated with Py-d_5, then ^{15}N-Py is added	~1800	~−400	15.1(2.3)	73.2(0.3)	~3600	~−2.7	~90
6) catalyst activated with ^{15}N-Py, then in n.a. Py is added	~1800	~−450	9.9(1.1)	70.0(0.3)	~3600	~−1.0	~90
7) catalyst activated with n.a. Py, then ^{15}N-Py is added	~1800	~−380	8.2(1.1)	69.9(0.3)	~3600	~−0.6	~90

[a]Note the activation sequence, which determines the axial non-exchangeable ligand of the activated Ir-hydride catalyst complex. See the SI for details. [b]Conducted with >90% *para*-H_2, while the rest of the data is collected using 65−75% *para*-H_2, resulting in ~30−40% lower signal enhancements compared with those shown in row 1. Note that the data for pairs 2 and 3, 4 and 5, and 6 and 7 were respectively collected on the same day at the same level of *para*-H_2 enrichment and stored in a pressurized aluminum cylinder as previously described (and thus should be directly comparable).[40]

interactions that would otherwise transfer hyperpolarization to the target spins; hence, the ^{14}N spins are effectively (self-)decoupled from the bound *para*-H_2.

Our previous theoretical model of SABRE-SHEATH, while appropriate for ^{15}N-enriched substrates, no longer applies for n.a. Py, and hence we present an amended theoretical model to describe the polarization transfer in the n.a. case. The original model invokes an AA′BB′ four spin system, where AA′ represents the parahydrogen-derived hydrides and BB′ represents the equatorial (exchangeable) ^{15}N spins depicted in Figure 3A. For this case, we originally derived that the

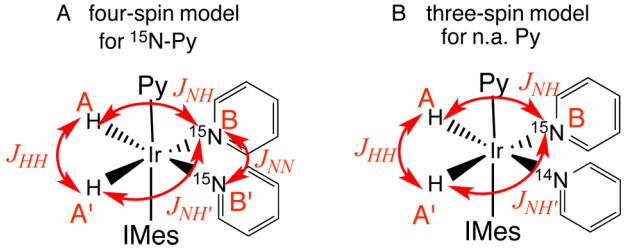

Figure 3. Spin systems used for analytical derivation of the resonance conditions for (A) ^{15}N-Py solutions and (B) n.a. Py solutions. In panel A, in addition to the displayed couplings, $J_{HN} = J_{H'N'}$ and $J_{HN'} = J_{H'N}$. Couplings to spins in axial positions are ignored because they generally are smaller than equatorial couplings and play a subordinate role. (Additionally, this site does not exchange with free substrate.)

magnetic field must be chosen such that at least one of the following resonance conditions are met

$$\Delta\nu_{HN} = |J_{HH} + J_{NN} - (J_{HN} + J_{HN'})/2| \quad (1)$$

$$\Delta\nu_{HN} = |J_{HH} - J_{NN}| \quad (2)$$

When these resonance conditions are met, then the N−H J couplings drive the hyperpolarization transfer; specifically, the term $(J_{HN} - J_{HN'})/2$ determines the rate of hyperpolarization transfer.

However, in the n.a. Py case, this spin system has to be adjusted because in 99.64% (= 100 − 0.36%) of species that contain one ^{15}N spin the adjacent equatorial species is a ^{14}N spin, not ^{15}N; therefore, we change our model to an AA′B three-spin system, where AA′ represents the parahydrogen-derived hydrides (as before) and B represents the ^{15}N spin. The ^{14}N spin can be ignored because as previously mentioned the strong quadrupolar interaction decouples the ^{14}N spin from the depicted spin systems.

In the SI we show that for the three-spin system the resonance condition is

$$\Delta\nu_{HN} = |J_{HH} - (J_{HN} + J_{HN'})/4| \quad (3)$$

In the three-spin system it is also the NH-J couplings that drive the hyperpolarization transfer; here it is specifically the term $(J_{HN} - J_{HN'})/(2\sqrt{2})$, which determines the rate of hyperpolarization transfer. Full derivation and additional details are given in the SI.

Next, we also performed conventional homonuclear ^{1}H-SABRE experiments. The ^{1}H signal enhancements, which are optimized in the milliTesla regime (Table 1) followed the general trend seen for ^{15}N SABRE-SHEATH, with signal enhancements being greater when the proton spin bath of to-be-hyperpolarized substrate was reduced. For example, $\varepsilon \approx (-)60$ was observed for Py-d_5 versus $\varepsilon \approx (-)4.2$ for n.a. Py, which is in agreement with previous studies.[15]

Because ^{14}N and other quadrupolar nuclei could have the potential to act as direct or indirect hyperpolarization sinks (e.g., polarization transfer from Ir-hydride protons to ^{14}N, D, etc. or from ^{15}N (after hyperpolarization transfer from *para*-H_2) to ^{14}N, D, etc.) at such low magnetic fields (analogous to interaction between ^{129}Xe and ^{131}Xe in xenon lattices[27]), and because the local molecular environment can significantly alter the ^{15}N effective T_1 in the microTesla field regime, ^{15}N SABRE-SHEATH of deuterated Py (Py-d_5) was studied as well as various mixtures of ^{15}N-Py and Py-d_5 with ^{15}N-Py and n.a. Py (Table 1). Note that the Py type (i.e., n.a. Py, Py-d_5, or ^{15}N-Py) used during the activation period determines the spin configuration of Py in the axial nonexchangeable position of the hexacoordinate Ir-hydride complex, whereas the abundance of the Py type in the mixture determines the most probable type of exchangeable Py in the two equatorial positions. (The corresponding most-probable configurations are summarized in the SI.) Deuteration of to-be-polarized ^{15}N-substrate had the most detrimental effect on microTesla ^{15}N effective T_1, a decrease from 5.5 ± 0.5 to 2.2 ± 0.1 s for n.a. Py versus Py-d_5 (row 1 vs row 2 of Table 1). A similar but slightly larger decrease (from $\varepsilon \approx (-)2900$ to $(-)850$) was observed for the corresponding SABRE-SHEATH ^{15}N enhancement values, indicating that the majority of deuterium-induced depolarization is due to indirect transfer, for example, from ^{15}N to ^{2}H.[28] However, the direct depolarization losses are likely to have a

DOI: 10.1021/acs.jpclett.5b00782
J. Phys. Chem. Lett. 2015, 6, 1961−1967

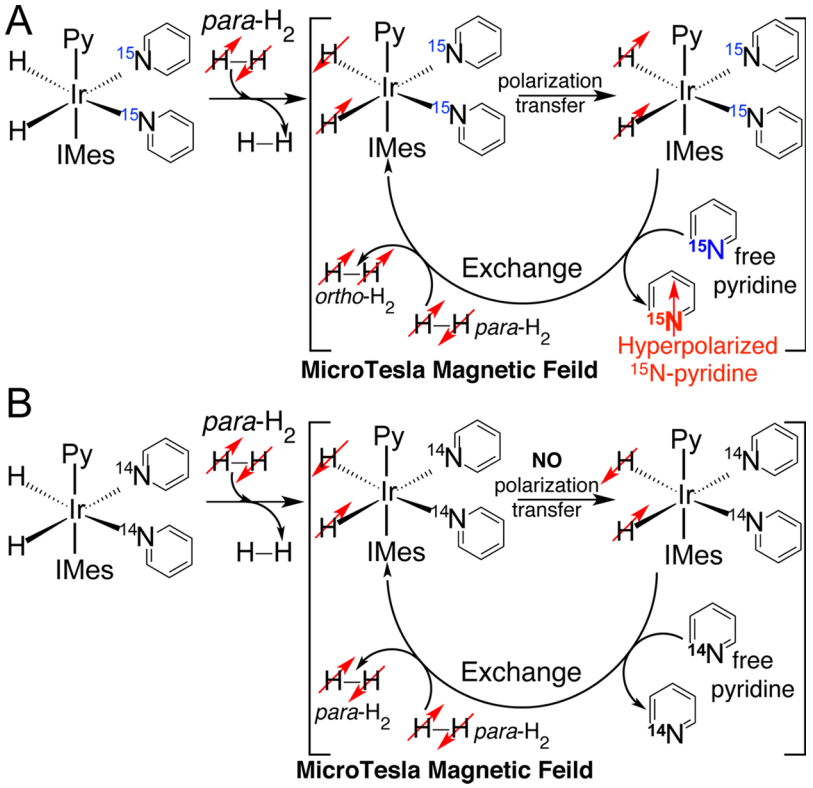

Figure 4. Diagrams of *para*-H_2 exchange and ^{15}N SABRE-SHEATH hyperpolarization in the absence (A) and in the presence (B) of ^{14}N-Py excess. Note that the exchange with ^{14}N-Py does not cause a significant reduction in the spin order of the *para*-H_2 pool. It should also be noted that both equatorial pyridines of the active complex undergo the chemical exchange with free Py in solution, while the axial pyridine (labeled as "Py") is not exchangeable.

significant contribution as well. For example, in cases when nondeuterated ^{15}N-Py was used in combination with Py-d_5, microTesla ^{15}N effective T_1 is actually *greater* when the catalyst is first activated with Py-d_5 versus that when catalyst is first activated with ^{15}N-Py, 15.1 ± 2.3 versus 10.1 ± 0.8 s (remembering that the activation order defines the non-exchangeable ligand in the axial position), but the ^{15}N signal enhancements were somewhat lower, $\varepsilon \approx (-)400$ vs $(-)520$, indicating that at least *some* polarization losses occurred on the hyperpolarized Ir-hydride due to the presence of deuterium in the catalyst structure. This particular finding at first seems to contradict recent studies where deuterium was incorporated in both catalyst[29] and exchangeable substrate[15,30] in the original homonuclear SABRE but can be explained by the different field regimes (microTesla vs several milliTesla) involved and by the fact that the previous efforts involved hyperpolarization of protons in exchangeable substrate instead of the present focus on ^{15}N nuclei polarized using ^{15}N SABRE-SHEATH.[17]

The effect of ^{14}N presence in the catalyst structure as a potential relaxation or polarization sink was studied by comparing two samples prepared using a mixture of ^{15}N-Py and n.a. Py (consisting mostly of ^{14}N-Py), rows 6 and 7 of Table 1. Activation of SABRE catalyst with ^{15}N-Py versus n.a. Py resulted in a slight increase in the microTesla ^{15}N effective T_1 (9.9 ± 1.1 s vs 8.2 ± 1.1 s) as well as the ^{15}N signal enhancement ($\varepsilon \approx (-)450$ vs $(-)380$), indicating that ^{14}N presence indeed can act as a weak relaxation or polarization sink, likely through contributions from both mechanisms; that is, direct transfer from hyperpolarized Ir-hydrides and from exchangeable ^{15}N-Py. To summarize, the above evidence advocates for avoiding the utilization of quadrupolar nuclei (e.g., deuterium and ^{14}N studied here) for ^{15}N SABRE-SHEATH hyperpolarization processes, whose presence can result in reduced hyperpolarization in microTesla fields.

As previously described, the ^{15}N SABRE-SHEATH of neat liquids is an advantageous tool for efficient hyperpolarization of ^{15}N spins, particularly at their low natural abundance level. One potential use is for rapid compound screening, which we demonstrate here on a series of picolines and lutidines shown in Figure 5. We find that the presence of a methyl group in position 2 or 6 results in no detectable ^{15}N hyperpolarization via SABRE-SHEATH, whereas the substituents in other positions result in ^{15}N signal enhancements levels similar to those of Py. The obvious explanation is that steric hindrance induced by the presence of methyl groups in ortho positions significantly alters the time scale of the SABRE exchange process or reduces the association constant.

We chose to examine picolines and lutidines because it was previously shown that pH-mediated protonation of N-heterocylic compounds can be useful for in vivo pH imaging using conventional proton-based nonhyperpolarized sensing, where the difference in ^{15}N chemical shift induced by the agent protonation can be useful for pH imaging provided that the agent's pK_a is in the physiologically relevant range.[31,32] ^{15}N centers of the Py class screened here were also identified as promising hyperpolarized pH sensors with potential biomedical application to noninvasively image local variances in tissue pH.[33] Unlike previously demonstrated pH imaging with hyperpolarized $H^{13}CO_3^-/^{13}CO_2$ that relies on the measurement of the ratio of two exchanging species,[34] pH imaging using hyperpolarized ^{15}N heterocycles relies on the modulation of ^{15}N chemical shift, which changes by up to 100 ppm between

DOI: 10.1021/acs.jpclett.5b00782
J. Phys. Chem. Lett. 2015, 6, 1961−1967

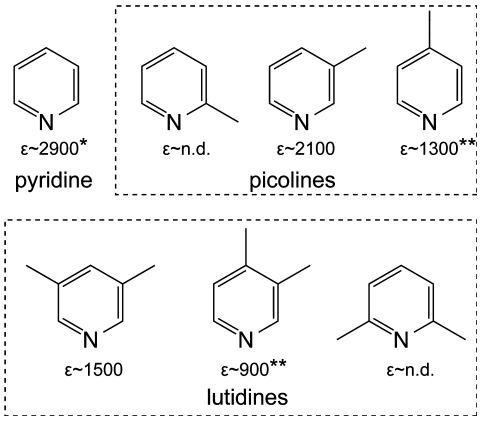

Figure 5. Maximum ^{15}N SABRE-SHEATH signal enhancements obtained for pyridine, picolines, and lutidines in neat liquids using ~45 mM catalyst concentration and naturally abundant levels of ^{15}N (~0.35%) under ~7 atm of *para*-H_2 pressure and flow rate of 100–120 sccm. Note that the value labeled with a single asterisk (*) corresponds to the optimized catalyst concentration of ~90 mM, the values labeled with double asterisks (**) correspond to the experiments conducted at 5 atm of *para*-H_2 and the flow rate of 60 sccm, and n.d. stands for none detected.

protonated and deprotonated states.[33,35] This feature offers a significant sensitivity advantage because only one species requires detection (i.e., ratiometric measurements are not needed), and low signal-to-noise ratio would not affect the accuracy of the measurement because the chemical shift reports on the pH. Moreover, hyperpolarized ^{15}N sites have significantly longer T_1 in aqueous media (>30 s)[33] compared with ^{13}C bicarbonate (~10 s),[34] which can also be a significant advantage for in vivo applications (especially relevant for applications involving cancer, given the known hallmarks of elevated glycolysis and mildly acidic microenvironments).[36,37] We note that the ^{15}N signal enhancements reported in Figure 5 are obtained in a nonoptimal setup, and thus they could potentially be increased through improved apparatus design, allowing for better access to the hyperpolarization source of *para*-H_2 (as well as reduced transit times to high field for detection). Moreover, the combination of heterogeneous SABRE[38] catalysts with the method presented here may allow preparation of pure hyperpolarized liquids because such solid-phase catalysts can be separated[38] and recycled.[39] Nevertheless, the reported ^{15}N signal enhancement values are already comparable to ^{15}N enhancements previously reported using dissolution DNP technology and a commercial DNP hyperpolarizer.[33] However, the method reported here achieves the steady-state maximum hyperpolarization level in <1 min without sophisticated equipment, versus ~2 h using expensive DNP hyperpolarizers.[33] It should be noted that unlike PHIP or DNP technologies, which have been successfully tested in vivo using relevant biomolecules, SABRE technology has not yet been demonstrated for in vivo use. SABRE for hyperpolarization of ^{15}N pH sensors can in fact directly lead to promising in vivo applications because the ^{15}N SABRE-SHEATH procedure is a relatively simple process and because in vivo pH sensors address an important metabolic biomedical question.

In conclusion, ^{15}N SABRE-SHEATH of neat liquids was successfully demonstrated on a model Py molecule and applied as a screening technique for mono- and dimethyl-substituted Py compounds shown to be promising for minimally invasive pH imaging.[33] Catalyst access to *para*-H_2 was found to be the limiting factor for achieving ^{15}N polarization levels beyond 1%. The ^{15}N SABRE-SHEATH process was found to be selective for utilizing the spin order of the *para*-H_2 spin bath for hyperpolarization of ^{15}N versus ^{14}N, enabling efficient hyperpolarization of neat liquids containing a naturally abundant level of ^{15}N. Deuterium and ^{14}N nuclei can act as direct and indirect hyperpolarization sinks and should be avoided or minimized where possible. While the NMR signal and polarization enhancements are relatively modest for ^{1}H SABRE of n.a. Py, (Py in milliTesla regime, $\varepsilon \approx 4$) and ^{15}N SABRE (^{15}N-Py in microTesla regime $\varepsilon \approx 33$) due to the finite capacity of the parahydrogen/Ir-hydride spin bath, the resulting payload of ^{15}N hyperpolarization (the product of agent concentration and its hyperpolarization) is more than doubled in this proof-of-principle demonstration compared with previous demonstrations of ^{15}N SABRE in methanol-d_4 solutions.

■ ASSOCIATED CONTENT

Supporting Information

Experimental details and T_1 simulations based on experimental data at microTesla and 9.4 T magnetic fields. The Supporting Information is available free of charge on the ACS Publications website at DOI: 10.1021/acs.jpclett.5b00782.

■ AUTHOR INFORMATION

Corresponding Author

*E-mail: eduard.chekmenev@vanderbilt.edu.

Funding

This work was supported by NSF under grants CHE-1058727, CHE-1363008, CHE-1416268, NIH 1R21EB018014, and 2R15EB007074 and by the DOD CDMRP breast cancer award W81XWH-12-1-0159/BC112431.

Notes

The authors declare no competing financial interest.

■ REFERENCES

(1) Nikolaou, P.; Goodson, B. M.; Chekmenev, E. Y. NMR Hyperpolarization Techniques for Biomedicine. *Chem.—Eur. J.* **2015**, *21*, 3156–3166.

(2) Ardenkjaer-Larsen, J. H.; Fridlund, B.; Gram, A.; Hansson, G.; Hansson, L.; Lerche, M. H.; Servin, R.; Thaning, M.; Golman, K. Increase in Signal-to-Noise Ratio of > 10,000 Times in Liquid-State NMR. *Proc. Natl. Acad. Sci. U. S. A.* **2003**, *100*, 10158–10163.

(3) Goodson, B. M. Nuclear Magnetic Resonance of Laser-Polarized Noble Gases in Molecules, Materials, and Organisms. *J. Magn. Reson.* **2002**, *155*, 157–216.

(4) Eshuis, N.; van Weerdenburg, B. J. A.; Feiters, M. C.; Rutjes, F. P. J. T.; Wijmenga, S. S.; Tessari, M. Quantitative Trace Analysis of Complex Mixtures Using SABRE Hyperpolarization. *Angew. Chem., Int. Ed.* **2015**, *54*, 1481–1484.

(5) Kurhanewicz, J.; Vigneron, D. B.; Brindle, K.; Chekmenev, E. Y.; Comment, A.; Cunningham, C. H.; DeBerardinis, R. J.; Green, G. G.; Leach, M. O.; Rajan, S. S.; et al. Analysis of Cancer Metabolism by Imaging Hyperpolarized Nuclei: Prospects for Translation to Clinical Research. *Neoplasia* **2011**, *13*, 81–97.

(6) Mugler, J. P.; Altes, T. A. Hyperpolarized ^{129}Xe MRI of the Human Lung. *J. Magn. Reson. Imaging* **2013**, *37*, 313–331.

(7) Golman, K.; in't Zandt, R.; Thaning, M. Real-Time Metabolic Imaging. *Proc. Natl. Acad. Sci. U. S. A.* **2006**, *103*, 11270–11275.

(8) Day, S. E.; Kettunen, M. I.; Gallagher, F. A.; Hu, D. E.; Lerche, M.; Wolber, J.; Golman, K.; Ardenkjaer-Larsen, J. H.; Brindle, K. M. Detecting Tumor Response to Treatment Using Hyperpolarized C-13

DOI: 10.1021/acs.jpclett.5b00782
J. Phys. Chem. Lett. 2015, 6, 1961–1967

Magnetic Resonance Imaging and Spectroscopy. *Nat. Med.* **2007**, *13*, 1382−1387.
(9) Comment, A.; Merritt, M. E. Hyperpolarized Magnetic Resonance as a Sensitive Detector of Metabolic Function. *Biochemistry* **2014**, *53*, 7333−7357.
(10) Nelson, S. J.; Kurhanewicz, J.; Vigneron, D. B.; Larson, P. E. Z.; Harzstark, A. L.; Ferrone, M.; van Criekinge, M.; Chang, J. W.; Bok, R.; Park, I.; et al. Metabolic Imaging of Patients with Prostate Cancer Using Hyperpolarized 1-C-13 Pyruvate. *Sci. Transl. Med.* **2013**, *5*, 198ra108.
(11) Adams, R. W.; Aguilar, J. A.; Atkinson, K. D.; Cowley, M. J.; Elliott, P. I. P.; Duckett, S. B.; Green, G. G. R.; Khazal, I. G.; Lopez-Serrano, J.; Williamson, D. C. Reversible Interactions with Para-Hydrogen Enhance NMR Sensitivity by Polarization Transfer. *Science* **2009**, *323*, 1708−1711.
(12) Atkinson, K. D.; Cowley, M. J.; Elliott, P. I. P.; Duckett, S. B.; Green, G. G. R.; Lopez-Serrano, J.; Whitwood, A. C. Spontaneous Transfer of Parahydrogen Derived Spin Order to Pyridine at Low Magnetic Field. *J. Am. Chem. Soc.* **2009**, *131*, 13362−13368.
(13) Eisenschmid, T. C.; Kirss, R. U.; Deutsch, P. P.; Hommeltoft, S. I.; Eisenberg, R.; Bargon, J.; Lawler, R. G.; Balch, A. L. Para Hydrogen Induced Polarization in Hydrogenation Reactions. *J. Am. Chem. Soc.* **1987**, *109*, 8089−8091.
(14) Bowers, C. R.; Weitekamp, D. P. Transformation of Symmetrization Order to Nuclear-Spin Magnetization by Chemical-Reaction and Nuclear-Magnetic-Resonance. *Phys. Rev. Lett.* **1986**, *57*, 2645−2648.
(15) Cowley, M. J.; Adams, R. W.; Atkinson, K. D.; Cockett, M. C. R.; Duckett, S. B.; Green, G. G. R.; Lohman, J. A. B.; Kerssebaum, R.; Kilgour, D.; Mewis, R. E. Iridium N-Heterocyclic Carbene Complexes as Efficient Catalysts for Magnetization Transfer from Para-Hydrogen. *J. Am. Chem. Soc.* **2011**, *133*, 6134−6137.
(16) Theis, T.; Truong, M.; Coffey, A. M.; Chekmenev, E. Y.; Warren, W. S. LIGHT-SABRE Enables Efficient in-Magnet Catalytic Hyperpolarization. *J. Magn. Reson.* **2014**, *248*, 23−26.
(17) Theis, T.; Truong, M. L.; Coffey, A. M.; Shchepin, R. V.; Waddell, K. W.; Shi, F.; Goodson, B. M.; Warren, W. S.; Chekmenev, E. Y. Microtesla SABRE Enables 10% Nitrogen-15 Nuclear Spin Polarization. *J. Am. Chem. Soc.* **2015**, *137*, 1404−1407.
(18) Truong, M. L.; Theis, T.; Coffey, A. M.; Shchepin, R. V.; Waddell, K. W.; Shi, F.; Goodson, B. M.; Warren, W. S.; Chekmenev, E. Y. ^{15}N Hyperpolarization by Reversible Exchange Using SABRE-SHEATH. *J. Phys. Chem. C* **2015**, *119*, 8786−8797.
(19) Zhivonitko, V. V.; Skovpin, I. V.; Koptyug, I. V. Strong ^{31}P Nuclear Spin Hyperpolarization Produced Via Reversible Chemical Interaction with Parahydrogen. *Chem. Commun.* **2015**, *51*, 2506−2509.
(20) Truong, M. L.; Shi, F.; He, P.; Yuan, B.; Plunkett, K. N.; Coffey, A. M.; Shchepin, R. V.; Barskiy, D. A.; Kovtunov, K. V.; Koptyug, I. V.; et al. Irreversible Catalyst Activation Enables Hyperpolarization and Water Solubility for NMR Signal Amplification by Reversible Exchange. *J. Phys. Chem. B* **2014**, *18*, 13882−13889.
(21) Vazquez-Serrano, L. D.; Owens, B. T.; Buriak, J. M. The Search for New Hydrogenation Catalyst Motifs Based on N-Heterocyclic Carbene Ligands. *Inorg. Chim. Acta* **2006**, *359*, 2786−2797.
(22) Barskiy, D. A.; Kovtunov, K. V.; Koptyug, I. V.; He, P.; Groome, K. A.; Best, Q. A.; Shi, F.; Goodson, B. M.; Shchepin, R. V.; Coffey, A. M.; et al. The Feasibility of Formation and Kinetics of NMR Signal Amplification by Reversible Exchange (SABRE) at High Magnetic Field (9.4 T). *J. Am. Chem. Soc.* **2014**, *136*, 3322−3325.
(23) van Weerdenburg, B. J. A.; Gloggler, S.; Eshuis, N.; Engwerda, A. H. J.; Smits, J. M. M.; de Gelder, R.; Appelt, S.; Wymenga, S. S.; Tessari, M.; Feiters, M. C.; et al. Ligand Effects of NHC-Iridium Catalysts for Signal Amplification by Reversible Exchange (SABRE). *Chem. Commun.* **2013**, *49*, 7388−7390.
(24) Radhakrishnan, K.; Ramachandran, P. A.; Brahme, P. H.; Chaudhari, R. V. Solubility of Hydrogen in Methanol, Nitrobenzene, and Their Mixtures - Experimental Data and Correlation. *J. Chem. Eng. Data* **1983**, *28*, 1−4.
(25) Herskowitz, M.; Wisniak, J.; Skladman, L. Hydrogen Solubility in Organic Liquids. *J. Chem. Eng. Data* **1983**, *28*, 164−166.
(26) Brunner, E. Solubility of Hydrogen in 10 Organic Solvents at 298.15-K, 323.15-K, and 373.15-K. *J. Chem. Eng. Data* **1985**, *30*, 269−273.
(27) Gatzke, M.; Cates, G. D.; Driehuys, B.; Fox, D.; Happer, W.; Saam, B. Extraordinarily Slow Nuclear-Spin Relaxation in Frozen Laser-Polarized Xe-129. *Phys. Rev. Lett.* **1993**, *70*, 690−693.
(28) We note that longer ^{15}N-effective T_1 in microTesla regime, in principle, would allow for longer hyperpolarization build-up (and greater steady-state ^{15}N hyperpolarization level) under the condition of rate-limited exchange on Ir-hydride catalyst (e.g., 5−10 exchanges per second) and substrate-to-catalyst ratio of >100:1.
(29) Ducker, E. B.; Kuhn, L. T.; Munnemann, K.; Griesinger, C. Similarity of SABRE Field Dependence in Chemically Different Substrates. *J. Magn. Reson.* **2012**, *214*, 159−165.
(30) Holmes, A. J.; Rayner, P.; Cowley, M. J.; Green, G. G. R.; Whitwood, A. C.; Duckett, S. B. The Reaction of an Iridium PNP Complex with Parahydrogen Facilitates Polarisation Transfer without Chemical Change. *Dalton Trans.* **2015**, *44*, 1077−1083.
(31) Gillies, R. J.; Raghunand, N.; Garcia-Martin, M. L.; Gatenby, R. A. Ph Imaging. *IEEE Eng. Med. Biol. Mag.* **2004**, *23*, 57−64.
(32) Bhujwalla, Z. M.; Artemov, D.; Ballesteros, P.; Cerdan, S.; Gillies, R. J.; Solaiyappan, M. Combined Vascular and Extracellular pH Imaging of Solid Tumors. *NMR Biomed.* **2002**, *15*, 114−119.
(33) Jiang, W.; Lumata, L.; Chen, W.; Zhang, S.; Kovacs, Z.; Sherry, A. D.; Khemtong, C. Hyperpolarized ^{15}N-Pyridine Derivatives as pH-Sensitive MRI Agents. *Sci. Rep.* **2015**, *5*, 9104.
(34) Gallagher, F. A.; Kettunen, M. I.; Day, S. E.; Hu, D. E.; Ardenkjaer-Larsen, J. H.; in't Zandt, R.; Jensen, P. R.; Karlsson, M.; Golman, K.; Lerche, M. H.; et al. Magnetic Resonance Imaging of pH in Vivo Using Hyperpolarized C-13-Labelled Bicarbonate. *Nature* **2008**, *453*, 940−U73.
(35) Alei, M.; Morgan, L. O.; Wageman, W. E.; Whaley, T. W. pH-Dependence of N-15 NMR Shifts and Coupling Constants in Aqueous Imidazole and 1-Methylimidazole - Comments on Estimation of Tautomeric Equilibrium Constants for Aqueous Histidine. *J. Am. Chem. Soc.* **1980**, *102*, 2881−2887.
(36) Gatenby, R. A.; Gillies, R. J. Why Do Cancers Have High Aerobic Glycolysis? *Nat. Rev. Cancer* **2004**, *4*, 891−899.
(37) Hanahan, D.; Weinberg, R. A. Hallmarks of Cancer: The Next Generation. *Cell* **2011**, *144*, 646−674.
(38) Shi, F.; Coffey, A. M.; Waddell, K. W.; Chekmenev, E. Y.; Goodson, B. M. Heterogeneous Solution NMR Signal Amplification by Reversible Exchange. *Angew. Chem., Int. Ed.* **2014**, *53*, 7495−7498.
(39) Shi, F.; Coffey, A. M.; Waddell, K. W.; Chekmenev, E. Y.; Goodson, B. M. Nanoscale Catalysts for NMR Signal Enhancement by Reversible Exchange. *J. Phys. Chem. C* **2015**, *119*, 7525−7533.
(40) Feng, B.; Coffey, A. M.; Colon, R. D.; Chekmenev, E. Y.; Waddell, K. W. A Pulsed Injection Parahydrogen Generator and Techniques for Quantifying Enrichment. *J. Magn. Reson.* **2012**, *214*, 258−262.

DOI: 10.1021/acs.jpclett.5b00782
J. Phys. Chem. Lett. 2015, 6, 1961−1967